Development of the first well-defined tungsten oxo alkyl derivatives supported on silica by SOMC: towards a model of WO_3/SiO_2 olefin metathesis catalyst

Etienne Mazoyer, Nicolas Merle, Aimery de Mallmann, Jean-Marie Basset, Elise Berrier, Laurent Delevoye, Jean-François Paul, Christopher P. Nicholas, Régis M. Gauvin and Mostafa Taoufik

Supplementary Information

General procedures

All experiments were carried out by using standard Schlenk and glove-box techniques. Solvents were purified and dried according to standard procedures. C_6D_6 (SDS) was distilled over Na/benzophenone and stored over 3Å molecular sieves. NpNa was prepared from NpLi following a procedure analogous to that used for BnK[1]. $WONp_3Cl$ (**1-Cl**) and supported [(≡SiO)W(=NAr)(=CH*t*Bu)Np] (**3**) were synthesized following the literature procedure.[2] [3] Propene was dried and deoxygenated before use by passing it through a mixture of freshly regenerated molecular sieves (3 A) and R-3-15 catalysts (BASF). $SiO_{2-(700)}$ was prepared from Aerosil silica from Degussa (specific area of 200 m^2 g^{-1}), which was partly dehydroxylated at 700 °C under high vacuum (10^{-5} Torr) for 15 h to give a white solid having a specific surface area of 190 m^2 g^{-1} and containing 0.7 OH nm^{-2}. Gas-phase analyses were performed on a Hewlett-Packard 5890 series II gas chromatograph equipped with a flame ionisation detector and an Al_2O_3/KCl on fused silica column (50 m X 0.32 mm). Elemental analyses were performed at the CNRS Central Analysis Department of Solaize (metal analysis) or in the LSEO (Dijon, for C, H analysis). IR spectra were recorded on a Nicolet 6700 FT-IR spectrometer by using a DRIFT cell equipped with CaF_2 windows. The samples were prepared under Ar within a glove-box. Typically, 64 scans were accumulated for each spectrum (resolution 4 cm^{-1}). Confocal Raman spectra were acquired using the 488nm line of a Ar-ion laser (Melles Griot). The excitation beam was focused on the sample by a 50X long working distance microscope and the scattered light was analyzed by an air-cooled CCD (Labram HR, Horiba Jobin Yvon). The fluorescence was subtracted from the spectra for clarity. Solution NMR spectra were recorded on an Avance-300 Bruker spectrometer. All chemical shifts were measured relative to residual ^1H or ^{13}C resonance in the deuterated solvent: C_6D_6, δ 7.15 ppm for ^1H, 128 ppm for ^{13}C. Solid-state NMR spectra were acquired on a Avance II 800 spectrometers (^1H: 800.13 MHz, ^{13}C: 201.21 MHz). For ^1H experiments, the spinning frequency was 20 kHz, the recycle delay was 5 s and 16 scans were collected using a 90° pulse excitation of 3 μs. The ^{13}C CP MAS experiment was obtained at a spinning frequency of 20 kHz, with a recycle delay of 5 s and 10312 scans were collected. Optimal resolution was achieved using the PISARRO decoupling scheme[4] at a RF field strength of 70 kHz and with a decoupling pulse unit of 45 μs, corresponding to $0.9^*\tau_R$ (where τ_R is the rotor period). The Hartmann-Hahn conditions were optimized with a ramped radio frequency (RF) field centered at 50 kHz applied on protons, while the carbon RF field was matched to obtain optimal signal. The contact time was set to 10 ms. The same CP and decoupling conditions were used for the acquisition of the two-dimensional HETCOR spectrum. The number of collected scans was limited to 688, with a recycling delay of 5s and 50 t_1 increments in the ^1H dimension, leading to a total experimental time of 48 hours. Chemical shifts were given in ppm with respect to TMS as external reference for ^1H and ^{13}C NMR. Procedures related to Extended X-ray Absorption Fine Structure Spectroscopy (EXAFS) are described in detail below.

Preparation and characterization of 1-Np

1-Cl (1.500 g, 3.34 mmol) was dissolved in 10 cm^3 of Et_2O and a solution of NpNa (0.314 g, 3.34 mmol) in 10 cm^3 of Et_2O was added dropwise in absence of light while stirring at -78°C. After one hour, the volatiles were removed *in vacuo*. Pentane was added and the reaction mixture was filtered to remove insoluble NaCl. Pentane was evaporated to afford a colourless oil. The crude material was distillated twice at 60°C under reduced pressure (3.10^{-5} Torr) to yield 0.570 g of pure product (35 % yield). ^1H NMR (δ, 295 K, C_6D_6, 300 MHz): 1.83 (6 H, s, $CH_2C(CH_3)_3$), 1.17 (24 H, s, $CH_2C(CH_3)_3$). ^{13}C NMR (ä, 295 K, C_6D_6, 75 MHz): 85.6 (s, $CH_2C(CH_3)_3$, ^{183}W satellites: $^1J_{W\text{-}C}$= 48.1 Hz), 34.5 (s, $CH_2C(CH_3)_3$), 32.9 (s, $CH_2C(CH_3)_3$). As the product was a heat, light and air sensitive oil, elemental analyses were not successful.

Figure S1: Compared ^1H and ^{13}C NMR spectra of **1-Cl** and **1-Np** (C_6D_6, 295K, ^1H: 300 MHz, ^{13}C: 75 MHz)

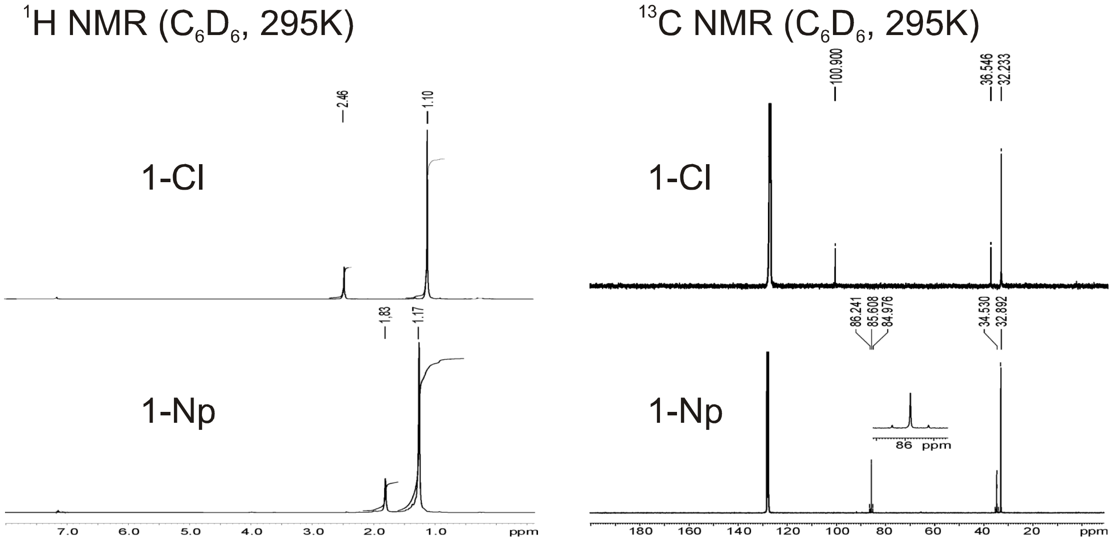

Preparation and characterization of 2

A mixture of **1-Np** (500 mg, 1.03 mmol) and SiO_{2-700} (2 g) in pentane (10 mL) was stirred at 25°C overnight. After filtration, the solid was washed 5 times with pentane and all volatile compounds were condensed into another reactor (of known volume) in order to quantify neopentane evolved during grafting. The resulting white powder was dried under vacuum (10^{-5} Torr). Analysis by gas chromatography indicated the formation of 403 μmol of neopentane during the grafting (0.9±0.1 NpH/W). Elemental analysis: W 4.1$\%_{wt}$ C 4.2$\%_{wt}$. ^1H MAS NMR (800 MHz) δ 1.93, 1.01 ppm. ^{13}C CP MAS NMR (200 MHz) δ 91, 34, 31 ppm.

Figure S2: Raman spectrum of **2**

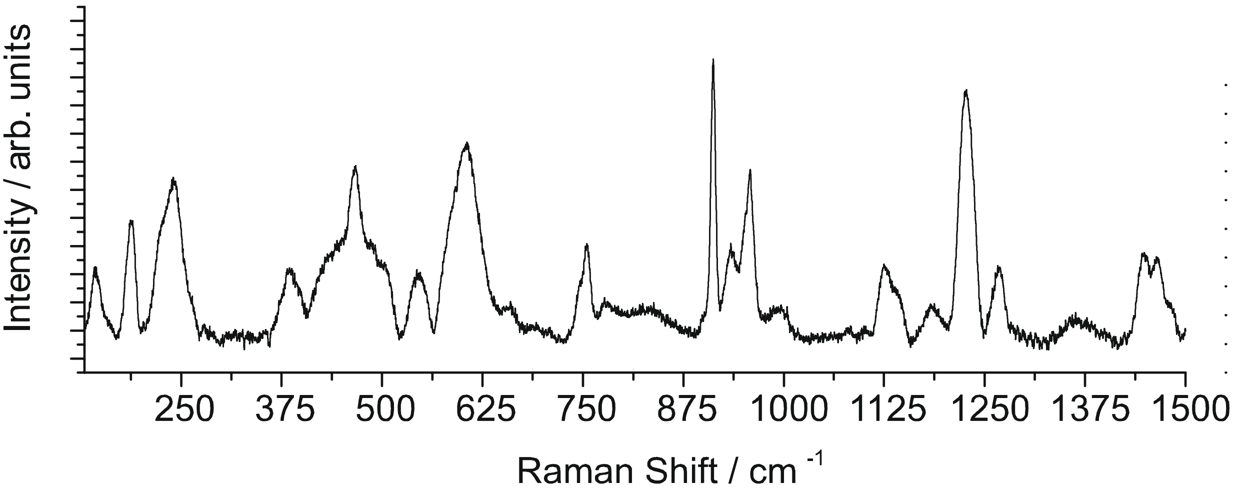

Figure S3: Solid-state NMR data (18.8T) of **2**: a) ^1H MAS, b) ^{13}C CP MAS and c) ^1H-^{13}C HETCOR CP MAS.

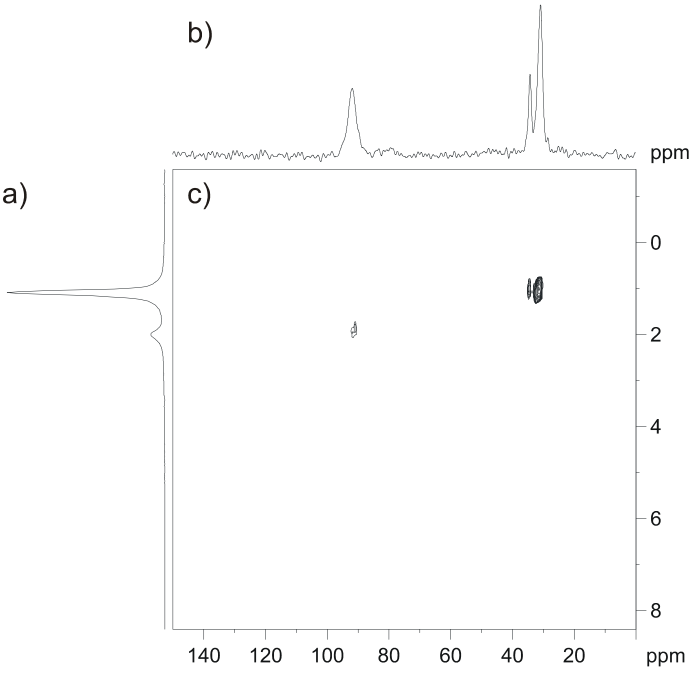

EXAFS characterization of 2.

X-ray absorption spectra were acquired at the SRS of the CCLRC in Daresbury (UK), using beam-line 9.3 (project # 50049), at room temperature at the tungsten L_{III} edge, with a double crystal Si(111) monochromator detuned 70% to reduce the higher harmonics of the beam (Figure S4). The spectra were recorded in the transmission mode between 10.05 and 11.45 keV. The supported W sample was packaged within a nitrogen filled dry box in a double air-tight sample holder equipped with kapton windows. This type of cell has already been used and proved to be very efficient for air-sensitive compounds. The spectra analyzed were the results of four such acquisitions and no evolution could be observed between the first and last acquisition. The data analyses were performed by standard procedures using in particular the program “Athena”[5] and the EXAFS fitting program “RoundMidnight”,[6] from the “MAX” package.

Figure S4: Tungsten L_{III}-edge k^3-weighted EXAFS (left) and corresponding Fourier transform (right) with comparison to simulated curves for the W-containing surface species in **2**. Solid lines: experimental; dashed lines: spherical wave theory.

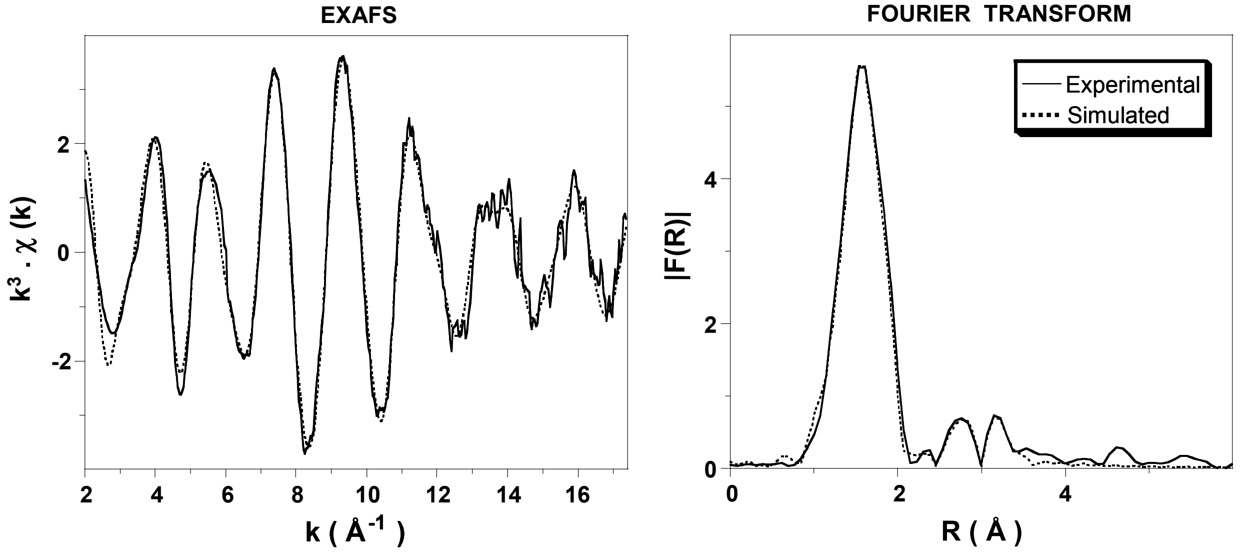

The program FEFF8 was used to calculate theoretical files for phases and amplitudes based on model clusters of atoms.[7] The value of the scale factor, $S_0^2 = 0.98$, was determined from the spectrum of the reference compound, a benzene solution of W(≡C-^{t}Bu)Np$_3$ (one carbon at 1.76(1) Å and three carbon atoms at 2.10(1) Å in the first coordination sphere). The refinements were performed by fitting the structural parameters N_i, R_i, σ_i and the energy shift, ΔE_0 (the same for all shells). The fit residue, ρ (%), was calculated by the following formula:

$$\rho = \frac{\sum_k [k^3\chi_{exp}(k) - k^3\chi_{cal}(k)]^2}{\sum_k [k^3\chi_{exp}(k)]^2} * 100$$

As recommended by the Standards and Criteria Committee of the International XAFS Society,[8] the quality factor, $(\Delta\chi)^2/\nu$, where ν is the number of degrees of freedom in the signal, was also calculated and considered. Results are gathered on Table S1.

Table S1. EXAFS parameters for **2**.[a] Errors generated by the EXAFS fitting program "RoundMidnight" are indicated between parentheses.

Type of neighbour	Number of neighbours	Distance (Å)	σ^2 (Å^2)
$\mathbf{W{=}\underline{O}}$	1.1(3)	1.71(1)	0.0018(9)
$\mathbf{W{-}\underline{O}}\mathrm{Si}\equiv$	1.2(6)	1.97(3)	0.002(2)
$\mathbf{W{-}\underline{C}}\mathrm{H_2CMe_3}$	3.1(15)	2.12(3)	0.003(2)
$\mathbf{W}\mathrm{{-}CH_2}\mathbf{\underline{C}}\mathrm{Me_3}$	3.1[b]	3.24(4)	0.004(3)
$\mathbf{W}\mathrm{{-}O}\mathbf{\underline{Si}}\equiv$	0.8(4)	3.60(4)	0.004(4)
$\mathbf{W{-}{-}\underline{O}}\mathrm{(Si\equiv)_2}$	0.8(7)	2.98(7)	0.007(8)

[a] Δk: [2.0–17.4 Å^{-1}] - ΔR: [0.7–3.6 Å]; $S_0^2 = 0.98$; $\Delta E_0 = 7.7 \pm 1.1$ eV (the same for all shells); Fit residue: $\rho = 3.4$ %; Quality factor: $(\Delta\chi)^2/\nu = 3.22$ ($\nu = 8 / 30$); three multiple scattering pathways have also been considered in the fit but not mentioned in this table. [b] Shell constrained to the parameter above. [c] From DFT calculations.

Figure S5: Ortep representation of $W_2O_3Np_6$ and selected distances in Å.[9]

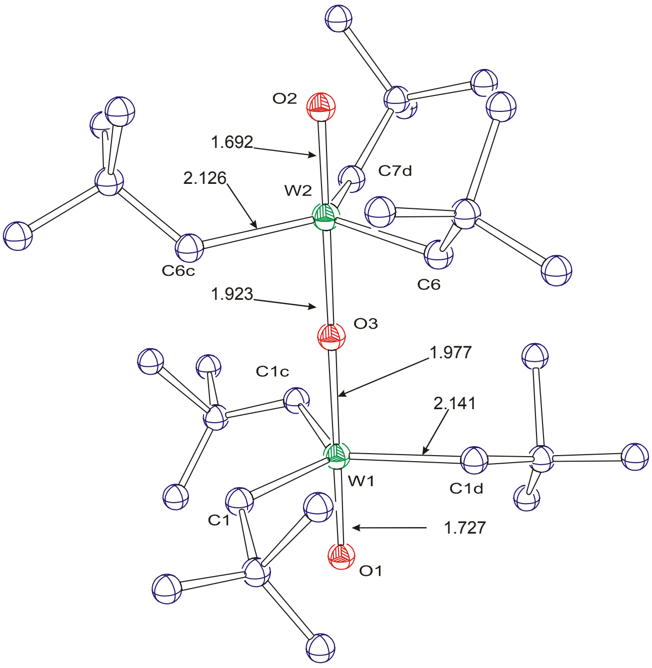

DFT calculations

All the calculations have been performed using the G03 program.[10] The geometries have been fully optimized without any symmetry constraints at the B3PW91 level with the Sddall basis set.

Figure S6: DFT calculated structure of **1-Np**

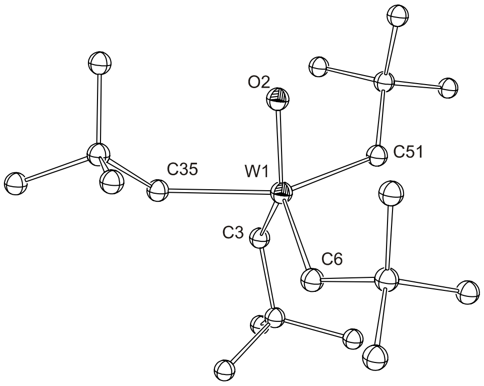

Table S2. DFT calculated atoms coordinates for **1-Np** (Å)

W	0.193352	0.089186	-0.037478
O	0.981308	0.638370	1.433261
C	-1.540279	0.123969	-1.481218
H	-2.173105	1.005457	-1.300710
H	-0.892176	0.424466	-2.339365
C	1.584001	-1.129014	-1.053099
H	1.310967	-0.987095	-2.117491
H	1.250281	-2.154900	-0.796270
C	-2.462680	-1.005662	-2.040594
C	-1.708650	-2.332074	-2.259893
H	-0.841291	-2.183423	-2.914930
H	-1.354178	-2.772111	-1.320960
H	-2.361688	-3.071347	-2.739282
C	-3.702017	-1.239546	-1.153018
H	-3.450829	-1.659807	-0.177099
H	-4.238991	-0.297699	-0.988172
H	-4.391240	-1.936063	-1.646540
C	-2.977760	-0.530686	-3.423783
H	-3.655866	-1.272075	-3.865718
H	-3.521254	0.416180	-3.328647
H	-2.144543	-0.375574	-4.119711
C	3.130598	-1.054796	-0.927448
C	3.630049	0.363572	-1.257830
H	3.279341	0.689760	-2.244845
H	3.288075	1.084746	-0.508058
H	4.725771	0.388156	-1.267358
C	3.589859	-1.444069	0.486865
H	3.196713	-0.749184	1.234463
H	3.256689	-2.456034	0.744099
H	4.684445	-1.426045	0.545574
C	3.732372	-2.049185	-1.945668
H	3.456477	-1.778291	-2.971641
H	4.826532	-2.052984	-1.878363
H	3.377236	-3.068237	-1.754289

C	-1.227037	-0.995535	1.157992
H	-2.125299	-0.364031	1.208960
H	-1.484553	-1.835962	0.492765
C	-0.920143	-1.565933	2.567110
C	0.392607	-2.368699	2.587246
H	0.385640	-3.156244	1.821935
H	1.253553	-1.718338	2.414381
H	0.527402	-2.854287	3.561051
C	-2.085536	-2.522622	2.920241
H	-1.950086	-2.933875	3.927926
H	-3.046629	-1.996005	2.895176
H	-2.137174	-3.362047	2.216152
C	-0.869569	-0.449225	3.623553
H	-0.067383	0.258454	3.404701
H	-1.820482	0.097200	3.654641
H	-0.696762	-0.876233	4.618858
C	0.197657	2.170786	-0.664493
H	1.273120	2.282677	-0.901624
H	-0.354210	2.245339	-1.607534
C	-0.233815	3.350669	0.250409
C	0.837254	3.670516	1.306959
H	1.023093	2.810584	1.953492
H	1.783141	3.949914	0.826586
H	0.514527	4.515006	1.928055
C	-0.414750	4.591488	-0.655670
H	-1.209820	4.430127	-1.393316
H	-0.679444	5.469874	-0.054873
H	0.511708	4.817761	-1.196279
C	-1.575506	3.049805	0.947009
H	-1.477686	2.216310	1.650832
H	-1.912709	3.925902	1.513907
H	-2.355782	2.800733	0.218771

Figure S7 : DFT calculated structure of **1-OSi$_{POSS-H}$** as a model of **2**

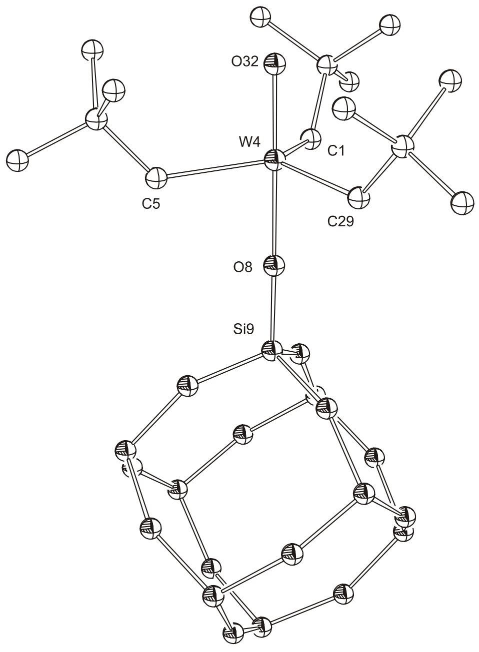

Table S3. DFT calculated atoms coordinates for **1-OSi**$_{\mathbf{POSS\text{-}H}}$ (Å)

C	2.789302	-1.230786	-1.751404
C	3.940137	-1.795133	-2.628358
C	3.271699	-2.633724	-3.755175
W	2.992079	0.000297	0.002714
C	2.738855	2.129311	-0.182194
C	3.863292	3.196915	-0.262251
C	4.762354	2.982581	-1.500247
O	1.002113	-0.030704	0.023174
Si	-0.645132	-0.036725	0.019625
O	-1.266801	-0.969313	-1.225299
Si	-2.532372	-1.616298	-2.119994
O	-3.457881	-0.327624	-2.678447
Si	-4.397849	1.048764	-2.453872
O	-5.674636	0.624146	-1.444932
Si	-6.305183	0.015172	-0.009714
O	-5.699707	-1.542056	0.180253
Si	-4.442707	-2.650537	0.318886
O	-3.491085	-2.504073	-1.060427
O	-1.274773	-0.647208	1.446546
Si	-2.549955	-1.063606	2.457374
O	-3.500869	-2.177029	1.629493
O	-1.275274	1.502534	-0.167760
Si	-2.512308	2.628227	-0.308955
O	-3.456512	2.168821	-1.623435
O	-3.478471	0.320115	2.685709
Si	-4.416242	1.602550	2.133965
O	-5.684547	0.948257	1.244259
O	-3.467474	2.495905	1.069766
C	2.828761	-0.931658	1.933181
C	3.998007	-1.355793	2.862262
C	3.355399	-1.983141	4.132262
O	4.746579	0.043075	-0.021341
C	4.765413	-0.662853	-3.279592
C	4.872287	-2.718192	-1.812123
C	4.851208	-0.139816	3.288645
C	4.898654	-2.414773	2.187991
C	3.157929	4.576900	-0.392726
C	4.727825	3.200163	1.018365
H	-2.071939	-1.611738	3.743505
H	-1.988972	4.000180	-0.473108
H	-4.949454	-4.028321	0.484464
H	-4.908509	2.435055	3.250715
H	-7.782455	0.026830	-0.016668
H	-4.879463	1.592791	-3.740193
H	-2.043260	-2.453079	-3.235164
H	2.177694	-2.068156	-1.369639
H	2.105681	-0.635694	-2.382599
H	2.158615	-0.242452	2.477212
H	2.210810	-1.817822	1.700423
H	5.289707	-0.074023	-2.523031
H	5.513502	-1.084619	-3.961767
H	4.120913	0.007984	-3.862536
H	5.400886	-2.157703	-1.036905
H	4.304219	-3.526756	-1.334013
H	5.619911	-3.177862	-2.469656
H	4.035399	-3.066662	-4.412506
H	2.679766	-3.455314	-3.334401
H	2.608006	-2.012039	-4.368072
H	5.377425	0.290037	2.432812

H	4.226835	0.639994	3.743667
H	5.600055	-0.443739	4.030050
H	4.313092	-3.289345	1.876047
H	5.399732	-2.000520	1.309498
H	5.668495	-2.760342	2.888750
H	2.742918	-2.855026	3.873179
H	4.134560	-2.309970	4.831654
H	2.716201	-1.257481	4.649296
H	2.098778	2.205113	-1.080328
H	2.073201	2.362433	0.667847
H	2.512481	4.772102	0.472143
H	3.901360	5.381251	-0.451294
H	2.539707	4.618496	-1.297607
H	4.105753	3.325672	1.914374
H	5.290818	2.268115	1.111812
H	5.446015	4.028630	0.990590
H	5.318474	2.045418	-1.422377
H	4.165913	2.960003	-2.421682
H	5.485734	3.802140	-1.590020

Figure S8: DFT calculated isomers of **1-OSi**$_{\text{POSS-H}}$

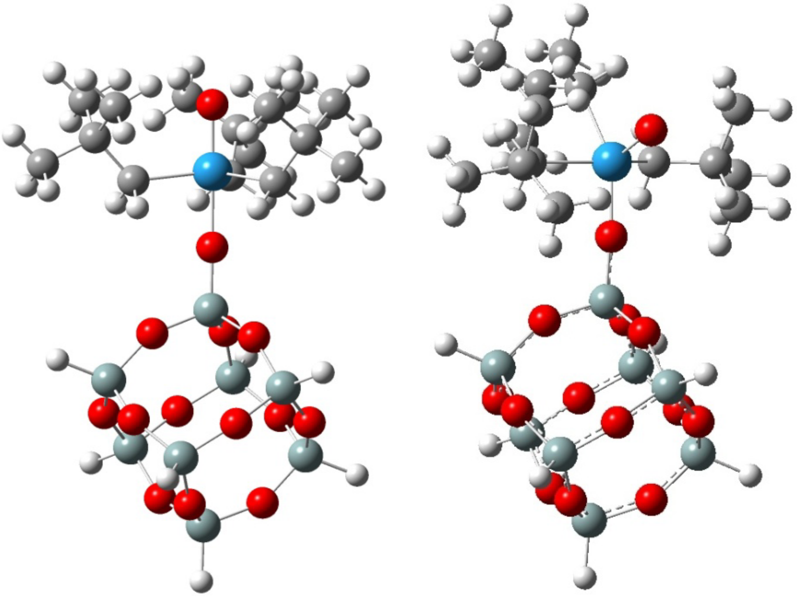

A **B**

The most stable isomer is A (ΔE=65 kJ), which consists of a distorted trigonal bipyramid with mutually trans oxo and surface siloxide as axial ligands, and with equatorial positions occupied by alkyl moieties.

Propene metathesis

Procedure in a batch reactor:

A mixture of solid **2** (100 mg) and propene (500 Torr, 40 equiv) were heated at 353K in a batch reactor of known volume. An aliquot was drawn and analyzed by gas chromatography after 24 hours.

Procedure in a flow reactor:

A stainless-steel half-inch cylindrical reactor that can be isolated from ambient atmosphere was charged with catalyst **2** (135 mg, % W = 4.2 %, 30 $mol_{C3H6}.mol_{W}^{-1}.min^{-1}$) or **3** (145 mg, % W = 3.5 %, 30 $mol_{C3H6}.mol_{W}^{-1}.min^{-1}$) in a glovebox. After connection to the gas lines and purging of the tubing, a 20 $ml.min^{-1}$ flow of propylene was passed over the catalyst bed at 80°C. Hydrocarbon products were analyzed online by GC (HP 8890 chromatograph fitted with an Al_2O_3/KCl 50 m x 0.32 mm capillary column, FID detector).

Figure S9: Compared selectivities of catalysts **2** (a) and **3** (b)

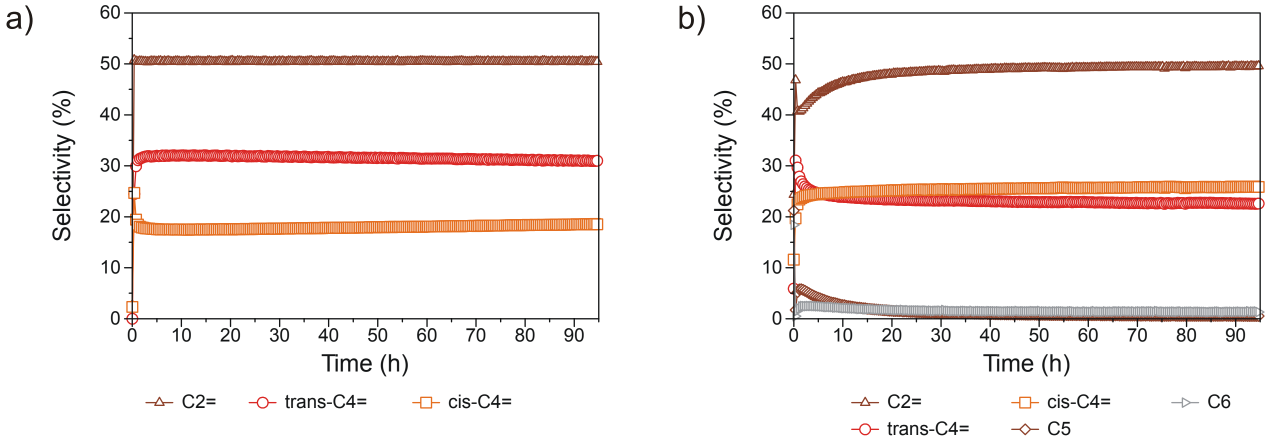

Figure S10: Evolution of isobutene selectivity over time for catalyst **3**

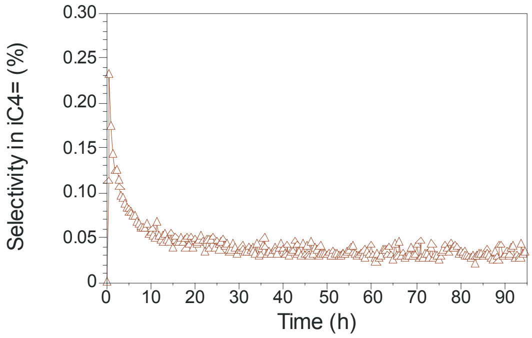

---

[1] M. Schlosser, J. Hartmann, *Angew. Chem.*, **1973**, *85*, 544; *Angew. Chem., Int. Ed. Engl.*, **1973**, *12*, 508.

[2] J. R. M. Kress, M. J. M. Russell, M. G. Wesolek, J. A. Osborn, *J. Chem. Soc.-Chem. Commun.* **1980**, 431.

[3] B. Rhers, A. Salameh, A. Baudouin, E. A. Quadrelli, M. Taoufik, C. Copéret, F. Lefebvre, J.-M. Basset, X. Solans-Monfort, O. Eisenstein, W. W. Lukens, L. P. H. Lopez, A. Sinha, R. R. Schrock, *Organometallics* **2006**, 25, 3554.

[4] M. Weingarth, P. Tekely, G. Bodenhausen, *Chem. Phys. Lett.*, **2008**, *466*, 247.

[5] B. Ravel, M. Newville, *J. Synch. Rad.* **2005**, *12*, 537.

[6] a) A. Michalovicz, '*Logiciels pour la Chimie*', S.F.C., Paris, **1991**, 102 ; b) A. Michalowicz, J. Moscovici, D. Muller-Bouvet, K. Provost, *Journal of Physics: Conference Series* **2009,** *190*, 012034.

[7] A. L. Ankudinov, B. Ravel, J. J. Rehr, S. D. Conradson, *Phys. Rev. B:* **1998**, *58*, 7565.

[8] Reports of the Standards and Criteria Committee of the International XAFS Society **2000:** http://ixs.iit.edu/subcommittee_reports/sc/

[9] I. Feinstein-Jaffe, D. Gibson, S. J. Lippard, R. R. Schrock, A. Spool, *J. Am. Chem. Soc.* **1984**, *106*, 6305.

[10] Gaussian G03, Revision D.0.1, M. J. Frisch, G. W. Trucks, H. B. Schlegel, G. E. Scuseria, M. A. Robb, J. R. Cheeseman, J. A. Montgomery, Jr., T. Vreven, K. N. Kudin, J. C. Burant, J. M. Millam, S. S. Iyengar, J. Tomasi, V. Barone, B. Mennucci, M. Cossi, G. Scalmani, N. Rega, G. A. Petersson, H. Nakatsuji, M. Hada, M. Ehara, K. Toyota, R. Fukuda, J. Hasegawa, M. Ishida, T. Nakajima, Y. Honda, O. Kitao, H. Nakai, M. Klene, X. Li, J. E. Knox, H. P. Hratchian, J. B. Cross, V. Bakken, C. Adamo, J. Jaramillo, R. Gomperts, R. E. Stratmann, O. Yazyev, A. J. Austin, R. Cammi, C. Pomelli, J. W. Ochterski, P. Y. Ayala, K. Morokuma, G. A. Voth, P. Salvador, J. J. Dannenberg, V. G. Zakrzewski, S. Dapprich, A. D. Daniels, M. C. Strain, O. Farkas, D. K. Malick, A. D. Rabuck, K. Raghavachari, J. B. Foresman, J. V. Ortiz, Q. Cui, A. G. Baboul, S. Clifford, J. Cioslowski, B. B. Stefanov, G. Liu, A. Liashenko, P. Piskorz, I. Komaromi, R. L. Martin, D. J. Fox, T. Keith, M. A. Al-Laham, C. Y. Peng, A. Nanayakkara, M. Challacombe, P. M. W. Gill, B. Johnson, W. Chen, M. W. Wong, C. Gonzalez, and J. A. Pople, Gaussian, Inc., Wallingford CT, 2004.